Environmental Research Communications

PAPER

Contributions of roads to surface temperature: evidence from Southern California

Ruth A Engel[1,*], **Adam Millard-Ball**[2] and **V Kelly Turner**[2]

[1] Department of Geography, University of California Los Angeles, United States of America
[2] Luskin School of Public Affairs, University of California Los Angeles, United States of America
[*] Author to whom any correspondence should be addressed.

E-mail: ruthengel@ucla.edu

Keywords: urban heat, land surface temperature, roads, streets, shade, cool pavement

OPEN ACCESS

RECEIVED
3 October 2022

REVISED
1 December 2022

ACCEPTED FOR PUBLICATION
14 December 2022

PUBLISHED
30 January 2023

Abstract

Planners often regard streets as targets for mitigating urban heat across cities by virtue of being abundant, publicly-owned, low-albedo, low-vegetation surfaces. Few studies, however, have assessed the role streets play in contributing to urban heat, and the scale of their effect relative to the built environment around them. We examine the relationship between road area and land surface temperature across a variety of biophysical regions through the urban areas of Los Angeles and San Bernardino Counties in Southern California. Our results show that wide streets have no consistent, detectable effect on urban heat. Rather, vegetation is the primary cooling mechanism for urban areas. In the absence of trees, concrete highways are the coolest surfaces, though particular hot or cool pockets (e.g., airports, industrial centers, parks) can dominate neighborhood temperature signatures. In considering LST mitigation strategies, these hotspots might outweigh the cumulative effects of road surface changes.

1. Introduction

Cities are hot in part because of impervious surfaces like buildings, roads, and parking lots. In most regions, urbanization replaces vegetated land with impervious surfaces, which decreases two key cooling factors: albedo and evapotranspiration. Urban heat planning, therefore, focuses on ways to increase albedo and vegetation to mitigate the effects of impervious surfaces on urban land. Heat produced by urban land cover is typically characterized as the surface urban heat island (SUHI), a regional phenomenon that causes cities to be, on average 1.5 °C warmer than surrounding undeveloped areas and is most pronounced at night (Oke 1982, Peng *et al* 2012). While the relative contributions of different surface materials are frequently studied through land *cover* analysis (Shiflett *et al* 2017), municipal planning decisions and policies are more typically organized around land *use* categories. The relative contributions of different land use categories to surface heat are less well understood.

One potential land use source of surface heat in urbanized regions is streets—large-scale, mostly low-albedo impervious surfaces that lack vegetation and shade (Taleghani *et al* 2016). The contribution of streets to urban heat is amplified by the large amount of land that they occupy—up to 30% in US cities such as New York (Manvel 1968, summarized in Meyer & Gómez-Ibáñez 2013, Millard-Ball 2022). Streets can influence the SUHI because of the effects of aspect ratio, width, and orientation on solar reflectivity and ventilation performance. At the same time, however, streets offer prime opportunities to mitigate urban heat—they are publicly owned resources upon which cities can site interventions without the need to incentivize private developers or land holders (Pomerantz *et al* 2003, Gago *et al* 2013, Lee *et al* 2018). For this reason, several cities have begun experimenting with cool pavement and urban tree planting programs to leverage streets as a public resource for mitigating surface heat (Maxwell *et al* 2018, Turner *et al* 2021, Ko *et al* 2022). These intervention programs focus on street trees and cool pavements as methods for increasing albedo and vegetation.

This study examines the relationship between street width and Land Surface Temperature (LST) across a variety of urban forms to examine how and where mitigation strategies might be best applied. We examine LST

across urban areas and evaluate the role of streets at both a regional and a neighborhood scale. We focus on communities in Los Angeles and San Bernardino Counties, California, which contain a mix of background biophysical conditions and built forms, and where policymakers have piloted the use of road surfaces to reduce urban heat through changes to vegetation or albedo (US EPA 2012, Garcetti 2021). These proposals follow a global trend of investment in cool pavement: Western Europe is pushing cool pavements, and pilot programs can be found in Tokyo, Athens, and Rome (Santamouris 2013, Municipality of Athens 2017, Moretti *et al* 2021). The United States government is also incentivizing cool pavement programs and several cities have followed suit (Wiltshire-Gordon 2020, FHA 2021, Garcetti 2021, SmartCities Connect 2021). We test the hypotheses that roads contribute to urban heat and that wider roads amplify those contributions. We further hypothesize that the impact of streets will vary based on the local physical context; hotter, more arid conditions will suppress the contribution of road widths to urban heat as will more intensively developed areas.

2. Mitigating urban heat on roads: vegetation, impervious surfaces, and land morphology

As conventionally described, a vegetation disparity across the urban environment creates a SUHI by producing hotter conditions in urban areas, especially developed downtown sectors, than surrounding undeveloped areas. The temperature disparity is largely driven by impervious surfaces like roads and buildings that absorb and slowly release heat throughout the day (Oke 1982, Rizwan *et al* 2008) and, depending on regional conditions, usually peaks during the early afternoon due to dependence on shortwave radiation (Shastri *et al* 2017, Lai *et al* 2018). Planning strategies often focus on mitigating the SUHI by reducing LST within urban cores.

The traditional SUHI has several limitations for urban planning. One shortcoming is that the direction of the relationship between urban land and surface temperature depends on background land and climate conditions. In hot desert climates, the typical SUHI pattern can be inverted: urbanized areas are often cooler than the background reference desert during the daytime, but warm up at night (Lazzarini *et al* 2015). Desert cities have substantially less dense vegetation and higher LST than temperate or forested cities, and a shallower diurnal heat cycle (Imhoff *et al* 2010). The inverse urban heat island is largely attributable to differences in vegetation and canopy cover: bare soil or sand in undeveloped desert areas is warmer than shaded or irrigated landscape in city centers (Shastri *et al* 2017, Mohamed *et al* 2021). Moreover, the relationship between urban land and temperature is heterogeneous within cities. This is problematic because developed areas, irrigated landscaping, and indigenous vegetation have distinct diurnal and annual NDVI, heat, and evapotranspiration cycles (Mini *et al* 2014, Hall *et al* 2016). These studies demonstrate that the direction and characteristics of the SUHI depend on the background land and climate conditions of the reference system.

Vegetation is also a primary mechanism for cooling spaces within cities: impervious surfaces and bare land are significantly warmer than vegetated areas, particularly in hot areas (He *et al* 2019). Shaded surfaces, and the air above those surfaces, are cooler than nearby unshaded impervious surfaces (Taleghani *et al* 2016). Tree cover, in particular, is effective in reducing surface temperature, but the mere presence of vegetation is sufficient to reduce localized surface and air temperature in comparison to a paved surface (Susca *et al* 2011, Adams and Smith 2014). In addition to shade, vegetation provides heat reduction through transpiration: as water is released into the atmosphere, sensible heat is converted to latent heat, reducing overall air temperature (Ballinas and Barradas 2016). This effect is heightened in arid climates with a high vapor pressure deficit that increases transpiration. A final pitfall in considering moderation of LST is the temptation to conflate the SUHI with the UHI, which reflects air temperature and is therefore affected by other phenomena, notably building morphology and wind (He *et al* 2020a, 2020b).

Urban heat varies with race and income as well as physical characteristics, in ways that exacerbate environmental injustices. For example, historically redlined neighborhoods show elevated surface temperatures of ~2.6 °C across the U.S. (Hoffman *et al* 2020, Wilson 2020). This trend holds for predominantly Black or Latinx neighborhoods, primarily due to a lack of vegetation (Harlan *et al* 2006, Dialesandro *et al* 2021). The need for LST intervention is unevenly distributed across urban areas.

Many cities have considered street trees as a strategy to mitigate urban heat given their large impacts on LST and their other benefits such as visual amenity and improved air quality (Mullaney *et al* 2015). Though tree planting is shown to be effective in reducing LST, many urban trees in Southern California are non-native and require constant irrigation, increasing water imports (Roman *et al* 2021). Indeed, angiosperm (broad-leaf) species comprise only 71% of trees in Los Angeles but contribute over 90% of tree transpiration (Litvak *et al* 2017). Landscaping comprises ~54% of residential water use in Southern California, and irrigation is both more prevalent and less responsive to mandatory drought-related water rationing in wealthy neighborhoods, which are shadier and cooler than low-income areas (Clarke *et al* 2013, Mini *et al* 2014). Because trees—particularly leafy, traditionally 'shady' trees—come with a cost, planners seek out alternate strategies for reducing LST.

Given these challenges, planners have also turned to road surface paint as a low-cost, easily-implemented method for mitigating LST. Roads, which are often constructed from dark asphalt, are logical targets for intervention: as continuous, often wide, impervious areas, they logically increase LST and radiant air temperature (Cheela *et al* 2021, Pomerantz *et al* 2003). Studies have tested potential reductions in LST from cool pavements, and found that higher-albedo surfaces are indeed cooler (Sodoudi *et al* 2014, Sen *et al* 2019). Citywide effects of cool pavement are mixed, however: as with any urban heat strategy that relies on increasing albedo, radiant temperature and midday temperature can increase even as incoming solar radiation decreases (Middell *et al* 2020, Erell *et al* 2014). Cool pavement pilot programs are assessing the effects of different surfaces within cities.

Cool pavements are often introduced inadvertently without regard to their albedo-increasing properties. For example, in Southern California, many of the widest roads are already concrete, which is classified as a cool pavement —studies have found that concrete with a higher cement content increases albedo regardless of the remaining composition (Lee *et al* 2002, Levinson and Akbari 2002, Sen *et al* 2019). This practice is likely to continue: because concrete sets rapidly and can include recycled tires for little expense, it continues to be the primary surface used in newly-repaired freeways (Caltrans 2002, CalRecycle 2020). Concrete is less prone to cracking than painted asphalt, and its construction can incorporate reflective materials to increase albedo (Cheela *et al* 2021). Concrete surfaces in Southern California can be used to understand existing cool pavements in context.

While most research has focused on the potential benefits and pitfalls of increasing cool pavement presence throughout cities (see for instance Santamouris 2013), several studies have examined specific aspects of the relationships between streets and heat. Microscale studies have compared road surfaces to one another, finding evidence of LST reduction with reflective pavements and shaded surfaces (Sodoudi *et al* 2014, Lee *et al* 2018). Others have evaluated the effects of building morphology, demonstrating that canyons and airflow can improve cooling at block and citywide scales (Johansson 2006, Giridharan *et al* 2007). Hoehne *et al* (2020) found increased sensible heat from combined car emissions and road surfaces across Phoenix. However, their LST readings seemed to correlate with imperviousness or bare ground, as opposed to irrigation. Yamazaki *et al* (2009) used very high resolution imagery (2 m) to examine LST, and found higher temperatures on impervious and road surfaces than in vegetated areas or water. However, they did not evaluate the effects of roads across a neighborhood or city scale, or in areas that are either highly vegetated or impervious.

There is substantial literature examining possible LST mitigation strategies across particular cities or neighborhoods (Deilami *et al* 2018, Mohammed *et al* 2020). However, few studies examine the relative impacts of vegetation or cool pavement strategies in distinct neighborhoods, rather than as a citywide panacea. Urban morphology can change at a neighborhood, or even a block scale within a city, affecting localized and citywide temperatures (Yuan *et al* 2020). Sodoudi *et al* (2014) examined a hybrid cool pavement and vegetation cooling model in Tehran, and found it to be more effective than either strategy in isolation. Middell *et al* (2020) found that cool pavement was not appropriate as a one-size-fits-all model, and should be applied with consideration of local context. To our knowledge, no studies have considered which areas might benefit from varying forms of LST mitigation.

3. Data and methods

3.1. Study area and case study selection

We examined the urbanized portion of Los Angeles and southwest San Bernardino Counties, California. We chose these counties because of their size, variety of climatic conditions and urban forms, and growing urban heat island (Dialesandro *et al* 2019, Ladochy *et al* 2021). Together, the counties are home to ~12 million people in over 100 incorporated cities, with substantial income disparities and a legacy of environmental injustice (Su *et al* 2009, US Census Bureau 2020). Our study area spans an east-west transect of California, covers elevation from sea level to >1000 m, and encompasses mediterranean and desert Koppen climate zones (Kesseli 1942). Coastal areas have a summertime marine layer, providing an overall cooling effect (Edinger 1959). The built form encompasses single-family homes, apartments, high-rise residential and office buildings, and industrial uses, and streets that range from large arterials to narrower streets built before the private car became dominant. While some of our predictive variables are hyperlocal, we examine LST at a neighborhood and citywide scale because it is well-suited for guiding interventions at regional, rather than block-level, scale (Turner *et al* 2022).

The primary urban area in our study region is the City of Los Angeles, a global megacity which contains a dense urban core, sprawling residential areas, and low-rise industrial zones. Notably, Los Angeles enforces a highway dedication ordinance requiring developers to physically widen streets to accommodate more traffic in exchange for building permits (Manville 2017). At the same time, the city considers streets to be a primary avenue for mitigating LST; in 2021 the Mayor's office announced an initiative to bring 200 blocks of cool pavement and 2,000 new trees to eight residential areas (Garcetti 2021).

In Southern California, we examine areas with both traditional and inverted SUHI. In coastal Los Angeles, heavily impervious urban areas (i.e. South and East LA) are warmer than the more vegetated mountainous or coastal neighborhoods (Dousset 1989, Hulley *et al* 2019). However, the eastern part of the state shows a reverse urban heat effect consistent with other hot desert cities (Shiflett *et al* 2017).

3.2. Data sources and calculations

We calculated LST at 30 m resolution using Landsat 8, parameterized with water vapor and emissivity from NCEP/NCAR reanalysis and ASTER imagery, for a 3-month composite of June, July, and August 2020 (Ermida *et al* 2020). To check our calculations, we validated our LST data using an alternative algorithm (Landsat Provisional LST) and data source (NASA ECOSTRESS LST readings). All three approaches are widely used in the literature, and we found agreement among the datasets. Thus, the remainder of the analysis uses the Landsat 8 imagery, so as to use a standard Landsat base for all variables and because of the ease of calculation in Google Earth Engine. Because we observed thermal LST, we were in effect observing the radiant temperature of tree canopy, shrubs, and grass in vegetated areas, rather than the temperature of the shaded pavement. Studies show, however, that shaded surfaces are significantly cooler than those in direct Sunlight (Barbierato *et al* 2019, Middell *et al* 2020).

Our data on street area, width, and class (highway, arterial, and residential street) use a novel method derived by Millard-Ball (2022), which derives street area and width from the voids between tax assessment parcels, and matches each void to OpenStreetMap (OSM) ways (maps available at [REDACTED]). Because right-of-way boundaries did not overlap exactly with 30 m pixels, we used two distinct measurements to assess street concentration within pixels. The first was street area, which we calculated by rasterizing street polygons at 1 m and summing the resulting 1 m pixels within each 30 m pixel. The second was street width, which we defined as the maximum width of any street that ran through each 30 m pixel.

We integrated additional data sources on urban form, vegetation, and demographics in order to incorporate other factors that prior studies show to have a strong influence on LST. We used building footprint polygons (Microsoft 2021) to calculate the largest building footprint within each 30 m pixel. While we examined clusters of 3×3 and 5×5 pixels to examine whether hotspots made surrounding areas warmer, we did not find a significant spatial spillover effect from streets. This null result may be due to the limited hyperlocal utility of LST as an indicator (Turner *et al* 2021).

We also examined Local Climate Zones (LCZ), a product created to show categories of land use, vegetation, and development for urban temperature studies (Stewart and Oke 2012). To explore questions of environmental justice, we classified pixels as a Disadvantaged Community or not according to the California Environmental Protection Agency's (EPA's) designation, which considers pollution burden, health outcomes, and vulnerability (CalEPA 2015).

To assess vegetation and land use, we examined Soil Adjusted Vegetation Index (SAVI) and albedo at 30 m using Landsat 8 data in Google Earth Engine (Roy et al 2014). A higher SAVI value indicates more greenness, with middling values corresponding to low vegetation and high values corresponding to forest. For each pixel's centroid, we calculated latitude, longitude, elevation, and distance from the Pacific Ocean (IHO 1953, Farr *et al* 2007).

For more specific information on data sources and calculations, see appendix A.

3.3. Regression

We use a linear regression model to test the association between LST (our dependent variable) and street area, while controlling for other predictors that may confound the relationship. These control variables consist of largest building footprint, SAVI, and albedo, all of which we standardize to mean zero and standard deviation one in order to be able to compare the magnitudes of the coefficients; disadvantaged community status as a binary variable; Local Climate Zone; and elevation and distance from the Pacific Ocean which we discretize into 10 bins in order to allow for nonlinear relationships. For an overview of other potential models, see appendix B.

3.4. Case studies

Our primary results are based on the urbanized areas of the two counties in our dataset. We complement these results with a more focused analysis of 14 case study communities (table 1; figure 1), in order to better understand the mechanisms that link street widths with urban heat. To do so, we compiled total street area and median LST, albedo, and SAVI in each neighborhood. We then selected each case study based on an extreme value strategy, choosing the areas with the maximum and minimum values for each variable. There was some overlap: the Pacific Palisades had the lowest median albedo and LST; Vernon had the lowest SAVI and highest LST; Colton had the highest albedo and lowest SAVI; and Grand Terrace had the least street area and lowest LST (figure 2).

We also included in our case study selection the three California Transformative Climate Communities (TCCs) within our study area: Ontario, Watts, and the San Fernando Valley (Transformative Climate

Table 1. Sample Neighborhoods; median LST, albedo, and SAVI; percentage of the neighborhood covered by streets; primary LCZ, median family income, and percent CalEPA designated environmentally disadvantaged area.

Neighborhood	County	Median LST	Median Albedo	Median SAVI	Percent Street Area	Primary LCZ	Median Family Income	Percent Envi. Disadvantaged
Chino Hills	SB	45.28	0.159	0.160	0.52	open lowrise	117,452	0.002
Colton	SB	45.56	0.194	0.125	0.60	open lowrise	60,372	83.68
Grand Terrace	SB	43.07	0.184	0.163	0.70	open lowrise	75,378	32.42
Hidden Hills	LA	33.33	0.183	0.275	0.91	large lowrise	165,336	0.00
Lancaster	LA	38.64	0.218	0.160	11.44	bush, scrub	60,799	3.12
Long Beach	LA	34.34	0.166	0.146	26.41	large lowrise	64,813	41.93
Ontario	SB	47.65	0.189	0.146	0.69	open lowrise	71,374	75.02
Pacific Palisades	LA	28.95	0.129	0.288	6.54	bush, scrub	220,362	0.00
Pacoima	LA	37.66	0.171	0.119	28.48	large lowrise	64,688	85.54
Rolling Hills	LA	29.75	0.158	0.297	4.00	large lowrise	186,818	0.00
Upland	SB	44.14	0.180	0.179	0.74	open lowrise	85,235	32.16
Vernon	LA	38.82	0.190	0.031	14.98	large lowrise	45,647	99.45
Watts	LA	36.16	0.164	0.136	30.03	large lowrise	44,470	94.79
Yucaipa	SB	46.90	0.176	0.170	12.30	open lowrise	84,654	0.00

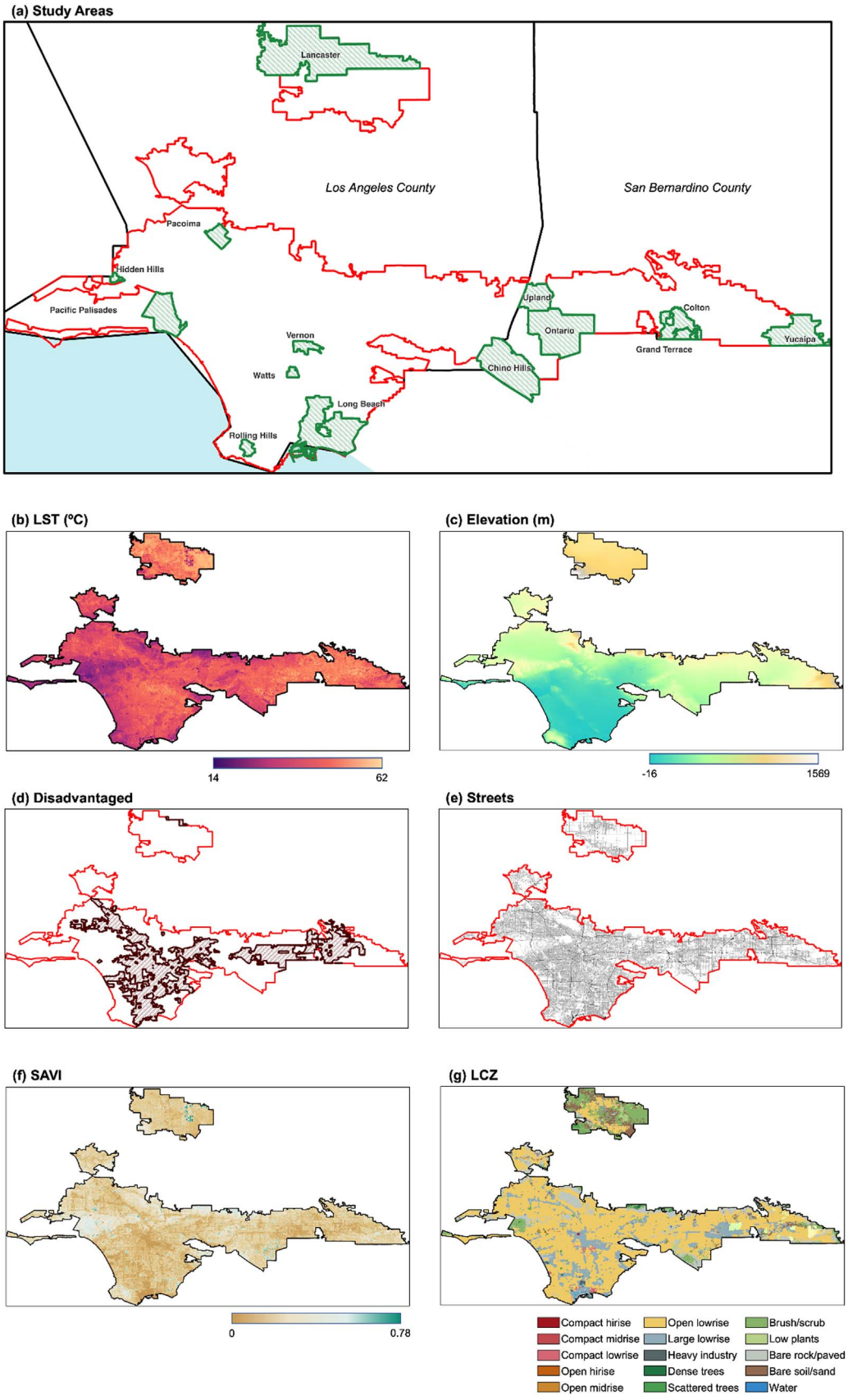

Figure 1. Spatial distribution of sample neighborhoods (a), LST (b) and selected contributing variables within the study area: Elevation (c), CalEPA Environmentally Disadvantaged Communities (d), Street networks (e), SAVI (f), and LCZs (g). Cooler areas are more mountainous and less developed, and often are coastal. Warmer areas are farther inland, and often are within large lowrise developments. Disadvantaged neighborhoods are, on average, hotter than non-disadvantaged neighborhoods.

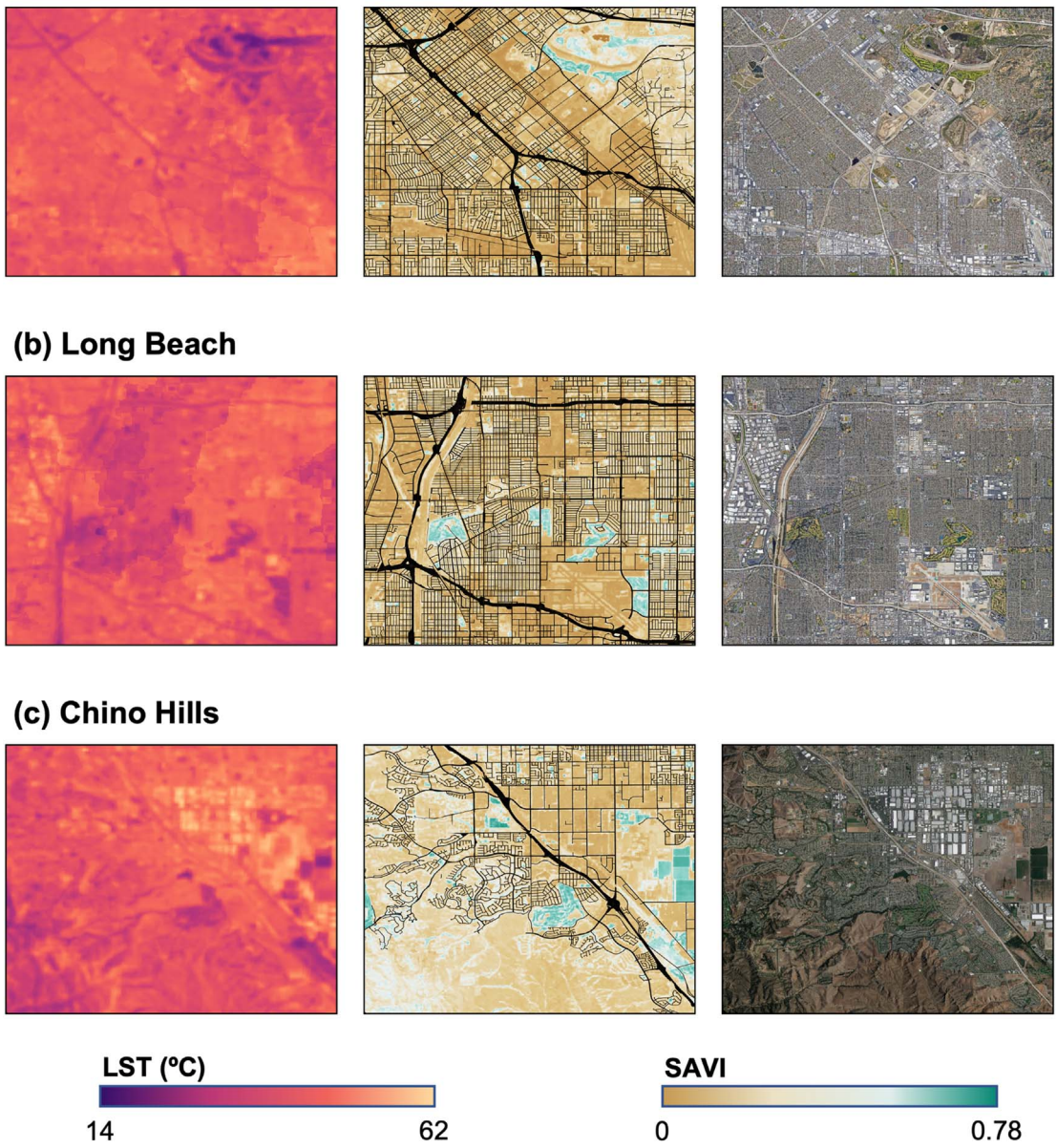

Figure 2. Temperature; SAVI and streets; and satellite imagery (Google 2021) for three sample neighborhoods. Pacoima is largely impervious and sits inland, in the San Fernando Valley. Highways are the coolest surfaces in the neighborhood. Long Beach is a diverse, coastal area, and generally cooler than other neighborhoods because of the summertime marine layer. A difference in temperature can be seen between residential and commercial areas. Chino Hills is wealthier and more vegetated, though it sits inland, in San Bernardino County. Several large warehouses, technically just outside the neighborhood, show the higher LST commonly visible in heavily industrial areas.

Communities 2021). For the purposes of this study, the San Fernando Valley area is called Pacoima, as almost all of the TCC zone is within that neighborhood. The TCCs are part of a California State initiative to reduce the legacy of redlining and environmental racism on underserved communities throughout the state via community-led action plans (Transformative Climate Communities 2021). We include the three TCCs because they represent long-marginalized areas with substantial environmental disadvantages.

4. Results

4.1. Effects of vegetation

We found that more vegetation, as expressed by higher SAVI, is universally correlated with lower LST. Notably, SAVI was the only tested variable without a sign change across all case study areas—that is, in each case, the regression coefficient is negative (table 2). Across the study area, SAVI also showed the strongest scaled correlations of any variable. We examined the signless magnitude of scaled correlations for street area, SAVI,

Table 2. Coefficients between street area and LST tend to be small, and they do not demonstrate a particular pattern. SAVI is the most noticeable predictor of LST, with cooling effects across all areas. Scaled regression coefficients for study area and all case studies shown. Variables are normalized so as to be directly comparable with one another. Model also includes Land Cover Zone, CalEPA Environmental Disadvantaged Status, and bins for elevation and ocean proximity to account for nonlinearity. Overall $R^2 = 0.767$. Variables that were correlated with streets were omitted in order to maintain the model's focus on streets as a possible predictor of LST. For more regression results, see appendix B.

		Scaled Correlations versus Temperature			
Neighborhood	County	Street Area	SAVI	Albedo	Largest Building Footprint
All Urbanized Areas		-0.05^{***}	-1.83^{***}	0.36^{***}	0.18^{***}
Ontario	SB	-0.19^{***}	-0.86^{***}	-0.06^{***}	0.44^{***}
Yucaipa	SB	-0.60^{***}	-2.10^{***}	0.07^{***}	-0.93^{***}
Colton	SB	-0.09^{***}	-0.51^{***}	-0.13^{***}	0.29^{***}
Chino Hills	SB	-0.15^{***}	-1.03^{***}	0.05^{***}	0.09^{***}
Upland	SB	0.10^{***}	-2.23^{***}	0.10^{***}	0.57^{***}
Grand Terrace	SB	-0.06	-1.05^{***}	0.19^{***}	-0.11^{*}
Vernon	LA	-0.12^{***}	-0.82^{***}	-0.22^{***}	0.70^{***}
Lancaster	LA	0.13^{***}	-0.98^{***}	-0.04^{***}	0.44^{***}
Pacoima	LA	0.34^{***}	-0.96^{***}	0.67^{***}	-2.96^{***}
Watts	LA	-0.11^{***}	-0.72^{***}	0.59^{***}	0.06^{***}
Long Beach	LA	0.09^{***}	-1.18^{***}	1.07^{***}	-0.23^{***}
Hidden Hills	LA	0.37^{***}	-1.69^{***}	2.01^{***}	1.07^{***}
Rolling Hills	LA	-0.14	-1.40^{***}	0.82^{***}	-2.05^{***}
Pacific Palisades	LA	0.05^{***}	-1.53^{***}	1.48^{***}	-0.38^{***}

$^{*}p < 0.05$. $^{**}p < 0.01$. $^{***}p < 0.001$.

albedo, and large building footprints, and found that SAVI's mean correlation with LST was 1.8% higher than the correlation of the next largest variable. SAVI was lower in environmentally-disadvantaged neighborhoods, which were >1 °C warmer on average than non-disadvantaged neighborhoods.

In examinations of specific areas, we found that higher SAVI correlated strongly with lower LST, but lower SAVI did not necessarily imply higher LST. Rather, areas with lower SAVI were more diverse, with a wider range of LST (figure 3). In some coastal areas (i.e. Long Beach) the effect of SAVI on LST was less visible, likely because of the 10:30 am collection time: Los Angeles experiences a summertime morning marine layer in coastal areas that can reduce LST (Edinger 1959).

4.2. Effects of roads

As a whole, roads had no consistent effect on LST in either the full dataset or our 14 case study neighborhoods. The null effect is apparent in our regression results in examinations of street width and area, both singly and in combination with other variables (table 2; figures 2 and 3). In some neighborhoods, more land devoted to streets is associated with increased temperatures, while in others it is associated with reduced temperatures, and in all cases the magnitude of the effect is small. Different model specifications with different choices of independent variables (appendix B) also fail to establish any consistent effect.

Within residential neighborhoods, vegetation was the dominant signature, and road area was a negligible factor in affecting LST (table 2). In highly impervious neighborhoods, road surface was often dwarfed by the presence of large buildings, which had a much more substantial impact on LST, with stronger correlations visible in table 2.

Highways were consistently the coolest road class, with lower LST values than arterials or residential streets. Across the study area, the median LST of highways was >1 °C cooler than other road surfaces (figure 4). In highly impervious areas with low SAVI, this effect is heightened; in Vernon, highways were 2.5 °C cooler than other road surfaces. In more highly vegetated areas such as the Pacific Palisades or Chino Hills, the effect is flattened, and most road surfaces have similar LST values.

In desertified or impervious areas, highways were often cooler than all other surrounding surfaces. Median highway temperature was 0.94 °C cooler than areas without roads across the study area, though this effect is skewed by the highly desertified San Bernardino areas: in the greener LA County, highways were 0.3 °C warmer than non-road surfaces. In extremely unvegetated areas, though, the effect is especially pronounced; Vernon's highways were 2.4 °C cooler than surrounding areas. In the neighborhood, the (concrete) highways showed a lower albedo than buildings (predominantly large warehouses) but a higher albedo than other roads. Most vegetated regions (i.e. Pacific Palisades, Rolling Hills) showed lower non-road LST than highway LST, but industrial or desertified regions (i.e. Pacoima, Colton) had lower highway LST (figure 4).

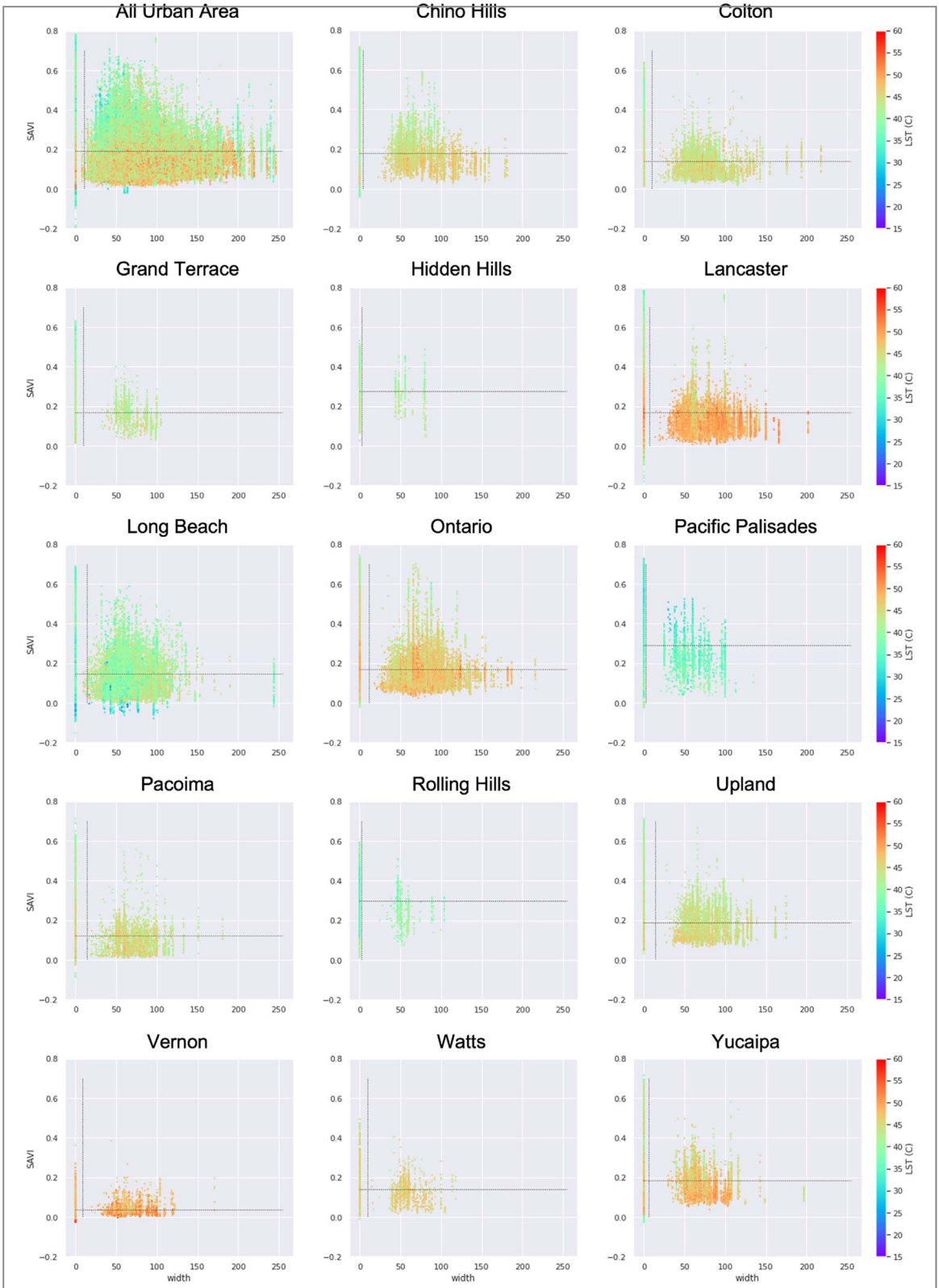

Figure 3. Most common street width (m) within each pixel and SAVI for each sample neighborhood. Colors represent summertime LST within a given pixel, and dashed lines are mean values for width and SAVI. Points for 'all urban area' plot come from a random selection of pixels to show a clear distribution without overcrowding. In both the study area as a whole and individual neighborhoods, SAVI is the primary moderator for LST: temperatures change along a vegetation gradient, but do not substantially differ in areas with narrow or wide streets. Areas with more vegetation (higher SAVI) are cooler, but areas with less vegetation (lower SAVI) are more diverse; low-SAVI areas are not universally warmer. In coastal neighborhoods (i.e. Hidden Hills, Long Beach, Pacific Palisades, and Rolling Hills) LST is lower across the board, a result of the summertime marine layer.

4.3. Vegetation and albedo

The primary cooling factor in most case study areas was vegetation, not albedo. Areas that lacked vegetation had the greatest variation in LST and correlations with albedo. This pattern was visible on road surfaces,

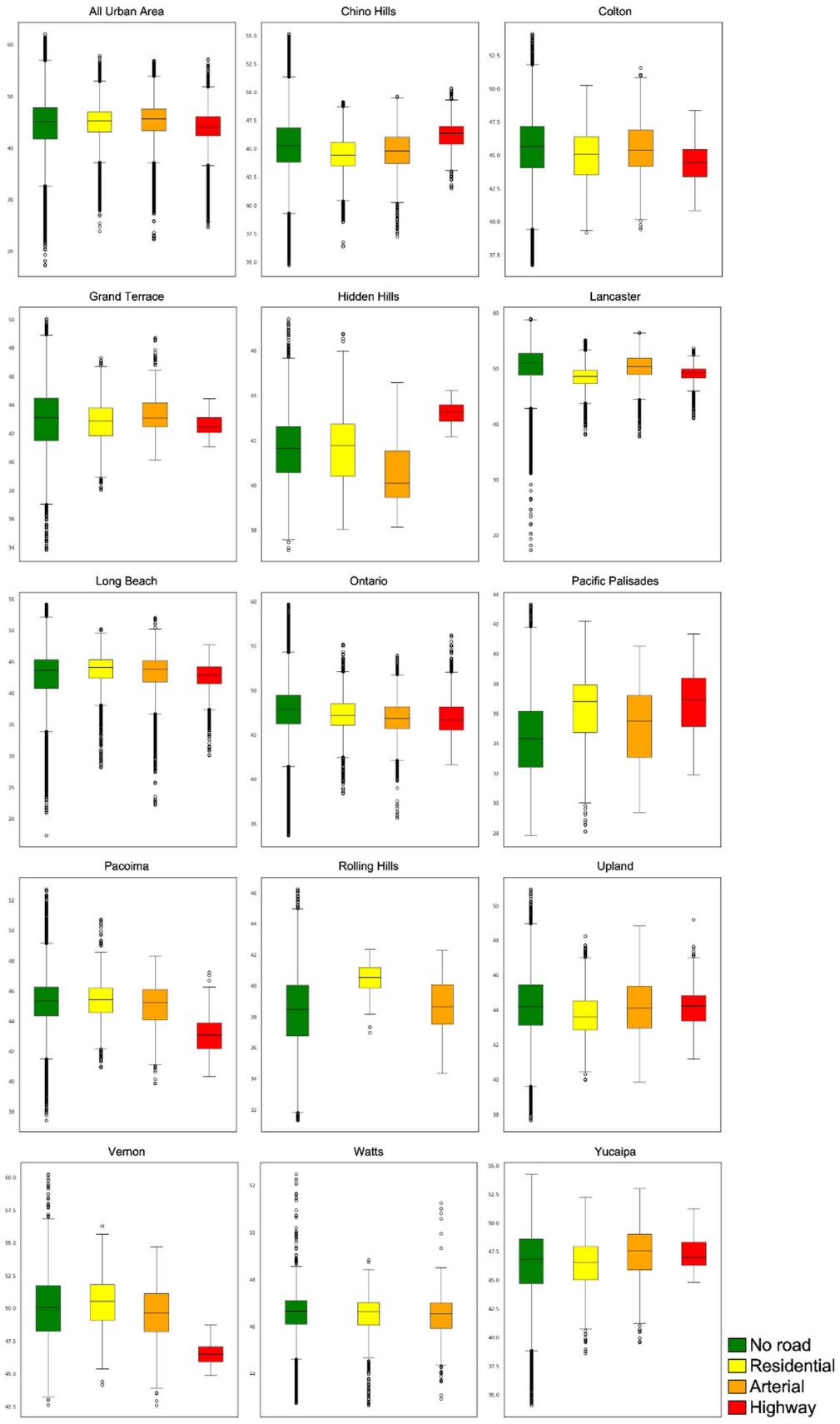

Figure 4. Distribution of LST (°C) of pixels with no roads (green), residential streets (yellow), arterials (orange), and highways (red) in each sample neighborhood. Rolling Hills and Watts have no highways. In wealthier neighborhoods with substantial vegetation (i.e. Chino Hills, Hidden Hills, Lancaster, and Pacific Palisades) the residential, high-SAVI areas are cooler than streets, and arterials with tree-lined medians can be especially cool. However, highways are the coolest streets in neighborhoods with diverse ground cover. In particularly impervious areas (i.e. Colton, Pacoima, and Vernon) highways are often the coolest areas overall.

where higher-albedo concretized highways showed lower LST than arterials and residential streets (figure 4).

In some areas, specific large-footprint industrial buildings with strong SAVI or albedo signatures dominated neighborhood effects (table 2). In homogeneous residential areas without major parks or barren sites (i.e. Upland, Watts, Pacoima), the relationship between albedo and LST was negative, as logic dictates. In case study areas with hotspots, some lower-albedo vegetation reduced overall LST (as in parks) or higher-albedo warehouses increased LST (figure 2).

5. Discussion

We found that SAVI was the strongest predictor of lower LST at pixel and neighborhood scales. This finding supports previous studies pointing to the dominant role of vegetation in mitigating urban heat, even in highly developed areas (Ballinas and Barradas 2016, Deilami *et al* 2018, Feng *et al* 2021). While urban vegetation does reduce LST, it is not always possible to rely on urban greening as a strategy for moderating SUHI. In Southern California's mediterranean and desert climates, for instance, increasing urban vegetation involves considering tradeoffs like water demand for irrigation and context factors such as species suitability (Mini *et al* 2014). In our study area specifically, many neighborhoods are dry and hot; grass and tree cover would not be feasible without a heavy investment in irrigation (Gober *et al* 2009). In Los Angeles, only 14% of the city's water is sourced locally (LADWP 2018). San Bernardino's primary aquifer is at a historic low and still losing water (SBVWCD 2022). Regional sustainability plans at both the city and county levels aim for reductions in water imports (Garcetti 2021). Our study region cannot rely on increased vegetation to reduce LST, so it is important to consider other options.

Our central question concerned whether streets contribute to urban heat and, accordingly, whether narrowing streets or introducing cool pavements would be a useful mitigation strategy. We found no consistent evidence that road surfaces in the study area increased LST relative to their surroundings. In accordance with a previous study conducted at the city-scale, we instead found that large, continuous surfaces, such as warehouses or parking lots, explained more variation in neighborhood-scale LST than streets (Liu and Zhang 2011). Urban context, therefore, appears to moderate the contributions of albedo and vegetation to surface temperature. For instance, parking lots in commercial and industrial areas occupy more land than streets, and they are typically surfaced in low-albedo black asphalt, likely amplifying their contributions to urban heat.

Within individual neighborhoods, overall morphology was important in the consideration of individual features (e.g. albedo or SAVI), echoing previous studies that emphasize the need for aligning LST mitigation strategies with local conditions (Sodoudi *et al* 2014, Feng *et al* 2021). Notably, we found that highways consistently had the lowest LST of all road surfaces, a result that confirms materials studies (Sen *et al* 2019, Cheela *et al* 2021). Because highways in our study area are primarily concrete, their higher albedo makes them cooler than asphalt. In shady neighborhoods, highways were the coolest streets, though not the coolest surfaces overall. In neighborhoods without shade, highways were the coolest of all surfaces. We also examined local morphology, and found its importance reflected in differences across land use types. In single-family residential neighborhoods with no parks, malls, or industrial sites, higher albedo was associated with lower LST. This effect was consistent regardless of climatic conditions. The presence of large warehouses, an airport, parks, or forested areas in many greener neighborhoods, however, led to a positive relationship between albedo and LST. The mechanism was imperviousness or building material rather than albedo: large white warehouses and bare ground are low LST hotspots, while parks and green spaces are cooler than their surroundings. Although we did not measure the effect of shade, we hypothesize that shade from nearby structures like buildings contributed to lower LST on some surfaces like warehouse roofs.

Between neighborhoods, localized conditions also played a role in determining LST trends. The study area was climatically and socioeconomically diverse at a neighborhood scale. Across Los Angeles County, we found that coastal areas had below-average LST and a weaker relationship between LST and SAVI likely due to a morning marine layer (figure 3). Local differences in vegetation and land use were equally important. Although the Pacific Palisades and Lancaster are both primarily classified within the 'brush, scrub' LCZ, the wealthy Palisades is heavily irrigated, while Lancaster has almost no irrigated urban canopy (Nowak *et al* 1996, Galvin *et al* 2019). LST mitigation strategies reflecting urban heterogeneity have been examined most notably in Hong Kong, where studies show that hotspots driving high LST are heterogeneously distributed throughout the city. There, proposed mitigation strategies are aimed at reducing LST in the areas of highest contribution or social vulnerability, rather than seeking to improve conditions citywide (Wong *et al* 2016, Hua *et al* 2021). Greening high-rise developments, providing shade for the elderly, and strategic additions of

pocket parks in coastal areas are all potential means of addressing a regional problem with targeted, local solutions (Giridharan *et al* 2008, Peng and Jim 2013, Peng and Maing 2021). Additionally, Hong Kong's varied topography and unique climate have led researchers to develop locally-determined 'seasons' for examination based on highly local conditions (Giridharan *et al* 2007, Chan 2011). In desert climates, strong seasonal effects might also be considered in constructing neighborhood-based LST mitigation strategies.

Our results suggest that effective mitigation of LST is dependent on local context. Future research could examine several ways in which neighborhood-scale LST varies both across and within neighborhoods. Other aspects of urban form, including parking lots, industrial sites, and parks, could be evaluated to assess relative contributions to LST. In some areas, there is potential for LST reduction co-benefits of investments in native plant cover and mixed green/gray shade as options for pedestrians. Areas with the least existing shade have the highest potential for LST moderation, particularly with respect to changes in albedo. Researchers might examine whether relationships between LST and urban morphology are functions of scale, shade, evapotranspiration, vegetation's albedo, or other factors. These analyses might also consider how each cooling mechanism, particularly shade, functions across a diurnal cycle: our analysis captures late morning conditions, before peak Sunlight, and further research might consider the effects of surfaces through the late afternoon and evening. A locally-driven LST mitigation program in Los Angeles might look similar to the model currently being piloted in Athens, Greece, using large, open, impervious spaces to improve microclimates (C40 2022). Strategies for SUHI mitigation rely on a highly targeted approach; planners and scientists alike are identifying areas of high LST or low heat resilience and addressing local conditions (Skoulika *et al* 2014, Mavrakou *et al* 2018, Mavrakou and Polydoros 2021). In instances where regional changes might be impractical, a suite of targeted, local interventions may create incremental improvements in surface heat mitigation or focus on different heat-related goals such as improving thermal comfort for pedestrians.

6. Conclusions

We examined LST across urban areas in Southern California with respect to mitigation potential along road surfaces, but found no consistent statistical relationship that would suggest that wide streets, as measured by greatest street width intersecting each pixel, are a major contributor to urban heat across urban area as a whole. Rather, we observed that vegetated areas are universally cooler than unvegetated areas, and that concrete highways, which have high albedo, can be cooler than other impervious, lower-albedo surfaces. While streets are often emphasized as the place to implement urban heat island mitigation policies such as cool surfaces, not all streets across all regions are measurably hotter than other urban uses, suggesting that policymakers might need to take a more targeted, context-specific approach, focusing on the individual neighborhoods where streets might contribute to surface heat due to a lack of vegetation and a high proportion of low-albedo asphalt surfaces. Municipalities might also focus on other features that contribute substantially to surface heat, including large parking lots or warehouses.

A more holistic approach might consider microclimates and local conditions, including shade, coastal effects, and dominant neighborhood land use. While streets comprise a large share of land use, they are often dwarfed by green spaces, parking lots, or buildings. There may be marginal gains from moving to cooler pavements, but the bigger drivers of high LST are often large, unbroken areas (i.e. parking lots or large buildings). Our local case study areas show a diverse view of LST, with various neighborhoods affected by climate, urban morphology, and land cover. As LST and SUHI mitigation become higher policy priorities, cities should avoid placing undue emphasis on publicly-owned streets without considering neighborhood context.

Acknowledgement

The authors are grateful for funding from the UCLA Luskin Center for Innovation.

Data availability statement

The data that support the findings of this study are openly available at the following URL/DOI: https://doi.org/ https://streetwidths.its.ucla.edu/map/.

Appendix A. Data sources and calculations

A.1. LST

Following Ermida (Ermida *et al* 2020), we calculated thermal LST at 30 m in Google Earth Engine using a statistical mono-window algorithm. We derived a Normalized Difference Vegetation Index (NDVI) and fractional vegetation cover from Landsat 8 cloud-free mosaics (Roy *et al* 2014). We obtained total column water vapor from 2.5 degree NCEP/NCAR reanalysis (Kalnay *et al* 1996) and bare ground emissivity from 100 m ASTER imagery (Hulley *et al* 2015). We then calculated thermal infrared emissivity and LST at Landsat 8 resolution.

To validate our calculations, we compared our summer 2020 LST to Landsat Provisional LST (30 m) and ECOSTRESS LST (38 × 69 m) from similar times of day (~6 pm UTC) (He *et al* 2019, Hulley *et al* 2019). Our data showed similar data distribution to both datasets.

A.2. Physical data

We calculated Soil Adjusted Vegetation Index (SAVI) and Albedo from Landsat 8 (30 m) using Google Earth Engine (Roy et al 2014). Because we examined specific, localized examples – often highly arid ones – in addition to the area as a whole, we selected SAVI to provide the most accuracy within semi-arid or arid regions (Vani *et al* 2017).

We derived elevation from a 30 m Shuttle Radar Topography Mission DEM (Farr *et al* 2007) in Google Earth Engine. Using a polygon of the Pacific Ocean's boundaries, we calculated distance from the coast (IHO 1953). We calculated latitude and longitude for each pixel centroid in Google Earth Engine.

A.3. Street and building data

We used street data from Millard-Ball (2022), obtained using GIS to derive road area from the spaces between plots of land. Each road segment corresponded to an OpenStreetMap (OSM) identifier, which was used to obtain street width and category. We aggregated OSM road categories into three: highway, arterial, and residential street. To calculate street area per 30 m pixel, we used Google Earth Engine to first rasterize the street polygons at 1 m, and then to aggregate them within each 30 m pixel. We obtained building footprints from Microsoft (2021), and identified the area of the largest building that intersected each 30 m pixel.

A.4. Land use data

To define our study area, we selected neighborhoods within city limits in San Bernardino County's Southwest corner, adjacent to Los Angeles County (SB County 2020). The majority of San Bernardino County is not urbanized, and we excluded small, individual cities (i.e. Barstow, Needles) surrounded by desert so as to examine a cohesive urban area. Within Los Angeles County, we selected incorporated neighborhoods; most of the excluded area is in the Angeles National Forest (USC 2017).

To examine land use, we used Land Cover Zones (LCZs) classified at 30 m for urban temperature analyses (Stewart and Oke 2012). The LCZs break down urban form based on vegetation and building density. In our study area, many of the less-developed urban areas are either chaparral or desert environments.

We obtained polygon data for Environmentally Disadvantaged Areas from CalEPA (2015), and rasterized them at 30 m. Environmentally Disadvantaged Areas represent the top 25% of the CalEnviroScreen 3.0 Assessment, which scored census tracts based on their economic condition as well as their climatic and pollution burdens. Several areas with very low populations but high pollution burdens are also included as Disadvantaged.

Appendix B. Regression data

In evaluating the regression model, we tested multiple scenarios to evaluate our choice of independent variables with respect to confounding effects, and to ensure that there was no substantial model calibration error. We found, no matter which independent variables were included or omitted, that Street Area and LST are not consistently correlated: the values of correlations are weak in comparison to other variables, and the models that do not account for environmental factors are weaker. Across the study area, Street Area and LST were slightly negatively correlated because of the reverse SUHI effect of the inland desert regions (table B1). However, the sign changed depending on the study area and the model specification (table 2).

Table B1. No matter which set of variables are used, Street Area is not a strong predictor of LST: coefficients tend to be small, and they do not have a consistent positive/negative correlation. SAVI is the most noticeable predictor of LST, with strong negative correlations. This table shows scaled regression coefficients for the entire study area. Variables are normalized so as to be directly comparable with one another. Models shown below include Street Area alone; Street Area and each primary variable individually; Street Area and each primary variable with all context variables; and all variables together with Street Area as quadratic and cubic. Other primary variables include SAVI, Albedo, and Largest Building Footprint. Context variables include Land Cover Zone, CalEPA Environmental Disadvantaged Status, and bins for elevation and ocean proximity to account for nonlinearity.

	Scaled Correlations versus Temperature					
Model	Street Area	SAVI	Albedo	Largest Building Footprint	Street Area (Quadratic)	Street Area (Cubic)
Street Area Alone ($R_2 = 9.9 \times 10^{-4}$)	0.14					
Street Area and SAVI ($R_2 = 0.28$)	−0.27	−2.47				
Street Area and Albedo ($R_2 = 0.11$)	0.28		1.55			
Street Area and Building Footprint ($R_2 = 0.02$)	0.18			0.62		
Street Area with Context ($R_2 = 0.51$)	0.15					
Street Area and SAVI with Context ($R_2 = 0.65$)	−0.09	−1.89				
Street Area and Albedo with Context ($R_2 = 0.53$)	0.21		0.58			
Street Area and Building Footprint with Context ($R_2 = 0.52$)	0.19			0.59		
Full Model; Street Area is Quadratic ($R_2 = 0.66$)	0.61	−1.83	0.40	0.17	−0.67	
Full Model; Street Area is Cubic ($R_2 = 0.66$)	−0.09	−1.84	0.40	0.17	1.15	−1.17

All values are significant at $^{***}p \leqslant 0.001$.

ORCID iDs

Ruth A Engel https://orcid.org/0000-0001-6183-1543
Adam Millard-Ball https://orcid.org/0000-0002-2353-8730
V Kelly Turner https://orcid.org/0000-0003-1383-5624

References

Adams M P and Smith P L 2014 A systematic approach to model the influence of the type and density of vegetation cover on urban heat using remote sensing *Landscape and Urban Planning* **132** 47–54
Ballinas M and Barradas V L 2016 Transpiration and stomatal conductance as potential mechanisms to mitigate the heat load in Mexico City *Urban Forestry & Urban Greening* **20** 152–9
Barbierato E *et al* 2019 Quantifying the impact of trees on land surface temperature: a downscaling algorithm at city-scale *European Journal of Remote Sensing* **52** 74–83
C40 2022 *Athens—C40 City Solutions Platform*
CalEPA 2015 SB 535 Disadvantaged Communities OEHHA https://oehha.ca.gov/calenviroscreen/sb535
CalRecycle 2020 Rubberized Asphalt Concrete (RAC). https://calrecycle.ca.gov/tires/rac
Caltrans 2002 CA Use of Fast-Setting Hydraulic Cement Concrete for Interstate Concrete Pavement Rehabilitation 990 https://fhwa.dot.gov/pavement/concrete/mcl9902.cfm2
Chan A L S 2011 Developing a modified typical meteorological year weather file for Hong Kong taking into account the urban heat island effect *Build. Environ.* **46** 2434–41
Cheela V R S *et al* 2021 Combating urban heat island effect—a review of reflective pavements and tree shading strategies *Buildings* **11** 93
Clarke L W *et al* 2013 The luxury of vegetation and the legacy of tree biodiversity in Los Angeles, CA *Landscape and Urban Planning* **116** 48–59
Deilami K *et al* 2018 Urban heat island effect: A systematic review of spatio-temporal factors, data, methods, and mitigation measures *Int. J. Appl. Earth Obs. Geoinf.* **67** 30–42
Dialesandro J *et al* 2021 Dimensions of thermal inequity: neighborhood social demographics and urban heat in the Southwestern U.S *International Journal of Environmental Research and Public Health* **18** 941
Dialesandro J M *et al* 2019 Urban heat island behaviors in dryland regions *Environ. Res. Commun.* **1** 081005
Dousset B 1989 AVHRR-derived cloudiness and surface temperature patterns over the Los Angeles area and their relationships to land use *Presented at the 12th CRSS* 2132–7
Edinger J G 1959 Changes in the depth of the marine layer over the Los Angeles Basin *J. Meteorol.* **16** 219–26
Erell E *et al* 2014 Effect of high-albedo materials on pedestrian heat stress in urban street canyons. Urban Climate, ICUC8 *The 8th International Conference on Urban Climate and the 10th Symposium on the Urban Environment* **10** 367–86
Ermida S L *et al* 2020 Google earth engine open-source code for land surface temperature estimation from the landsat series *Remote Sensing* **12** 1471
Farr T G *et al* 2007 The shuttle radar topography mission *Rev. Geophys.* **45**
Feng R *et al* 2021 Urban ecological land and natural-anthropogenic environment interactively drive surface urban heat island: An urban agglomeration-level study in China *Environ. Int.* **157** 106857
FHA 2021 Pavement Thermal Performance And Contribution To Urban And Global Climate - References - Sustainable Pavement Program - Sustainability - Pavements - Federal Highway Administration. https://fhwa.dot.gov/pavement/sustainability/articles/pavement_thermal.cfm
Gago E J *et al* 2013 The city and urban heat islands: A review of strategies to mitigate adverse effects *Renew. Sustain. Energy Rev.* **25** 749–58
Galvin M *et al* 2019 *Los Angeles County Tree Canopy Assessment* Center for Urban Resilience Reports
Garcetti E 2021 Mayor Garcetti kicks off second phase of 'Cool Streets LA' programOffice of Los Angeles Mayor Eric Garcetti https://lamayor.org/mayor-garcetti-kicks-second-phase-cool-streets-la-program
Giridharan R *et al* 2007 Urban design factors influencing heat island intensity in high-rise high-density environments of Hong Kong *Build. Environ.* **42** 3669–84
Giridharan R *et al* 2008 Lowering the outdoor temperature in high-rise high-density residential developments of coastal Hong Kong: The vegetation influence *Build. Environ.* **43** 1583–95
Gober P *et al* 2009 Using watered landscapes to manipulate urban heat island effects: how much water will it take to cool phoenix ? *Journal of the American Planning Association* **76** 109–21
Google 2021 Map Data
Hall S J *et al* 2016 Convergence of microclimate in residential landscapes across diverse cities in the United States *Landscape Ecol* **31** 101–17
Harlan S L *et al* 2006 Neighborhood microclimates and vulnerability to heat stress *Social Science & Medicine* **63** 2847–63
He B J *et al* 2019 An approach to examining performances of cool/hot sources in mitigating/enhancing land surface temperature under different temperature backgrounds based on landsat 8 image *Sustainable Cities and Society* **44** 416–27
He B J *et al* 2020a Relationships among local-scale urban morphology, urban ventilation, urban heat island and outdoor thermal comfort under sea breeze influence *Sustainable Cities and Society* **60** 102289
He B J *et al* 2020b Urban ventilation and its potential for local warming mitigation: A field experiment in an open low-rise gridiron precinct *Sustainable Cities and Society* **55** 102028
Hoehne C G *et al* 2020 Urban heat implications from parking, roads, and cars: a case study of metro phoenix *Sustainable and Resilient Infrastructure* **0** 1–19
Hoffman J S *et al* 2020 The effects of historical housing policies on resident exposure to intra-urban heat: a study of 108 US urban areas *Climate* **8** 12
Hua J *et al* 2021 Spatiotemporal assessment of extreme heat risk for high-density cities: A case study of Hong Kong from 2006 to 2016 *Sustainable Cities and Society* **64** 102507
Hulley G *et al* 2019 New ECOSTRESS and MODIS land surface temperature data reveal fine-scale heat vulnerability in cities: a case study for LA county, California *Remote Sensing* **11** 2136
Hulley G C *et al* 2015 The ASTER global emissivity dataset: mapping earth's emissivity at 100 meter spatial scale *Geophys. Res. Lett.* **42** 7966–76

IHO 1953 Limits of oceans and seas *IHO Special Publication* **3** 1–38
Imhoff M L *et al* 2010 Remote sensing of the urban heat island effect across biomes in the continental USA *Remote Sens. Environ.* **114** 504–13
Johansson E 2006 Influence of urban geometry on outdoor thermal comfort in a hot dry climate: A study in Fez, Morocco *Build. Environ.* **41** 1326–38
Kalnay E *et al* 1996 The NCEP/NCAR 40-year reanalysis project *Bull. Am. Meteorol. Soc.* **77** 437–72
Kesseli J E 1942 The climates of California according to the Köppen classification *Geographical Review* **32** 476–80
Ko J *et al* 2022 Measuring the impacts of a real-world neighborhood-scale cool pavement deployment on albedo and temperatures in Los Angeles *Environ. Res. Lett.* **17** 044027
Ladochy S *et al* 2021 Los Angeles' urban heat island continues to grow: urbanization, land use change influences *J. Urban Environ. Eng.* **15** 103–16
Lai J *et al* 2018 Identification of typical diurnal patterns for clear-sky climatology of surface urban heat islands *Remote Sens. Environ.* **217** 203–20
Lazzarini M *et al* 2015 Urban climate modifications in hot desert cities: The role of land cover, local climate, and seasonality *Geophys. Res. Lett.* **42** 9980–9
Lee E B *et al* 2002 Case study of urban concrete pavement reconstruction on interstate 10 *J. Constr. Eng. Manage.* **128** 49–56
Lee S *et al* 2018 Analyzing thermal characteristics of urban streets using a thermal imaging camera: a case study on commercial streets in Seoul, Korea *Sustainability* **10** 519
Levinson R and Akbari H 2002 Effects of composition and exposure on the solar reflectance of portland cement concrete *Cem. Concr. Res.* **32** 1679–98
Litvak E *et al* 2017 Evapotranspiration of urban landscapes in Los Angeles, California at the municipal scale *Water Resour. Res.* **53** 4236–52
Liu L and Zhang Y 2011 Urban heat island analysis using the landsat TM Data and ASTER data: a case study in Hong Kong *Remote Sensing* **3** 1535–52
Manville M 2017 Automatic street widening: Evidence from a highway dedication law *Journal of Transport and Land Use* **10** 375–93
Manvel A D 1968 *Land use in 106 large cities*12Three Land Research Studies, prepared for the consideration of the National Commission on Urban Problems
Mavrakou T *et al* 2018 Recognition of thermal hot and cold spots in urban areas in support of mitigation plans to counteract overheating: application for Athens *Climate* **6** 16
Mavrakou T and Polydoros A 2021 Assessing Urban Resilience to Thermal Risk: An Application for Athens, Greece *IJESNR* **29** 1–3
Meyer J R and Gómez-Ibáñez J A 2013 *Autos, Transit, and Cities* (Cambridge, MA: Harvard University Press)
Maxwell K *et al* 2018 Built environment, urban systems, and cities. impacts, risks, and adaptation in the united states: fourth national climate *Assessment* **2** 438–78
Microsoft 2021 *Building Footprints* (Microsoft)
Middell A *et al* 2020 Solar reflective pavements—A policy panacea to heat mitigation ? *Environ. Res. Lett.* **15** 064016
Millard-Ball A 2022 The width and value of residential streets *Journal of the American Planning Association* **88** 30–43
Mini C *et al* 2014 Estimation of residential outdoor water use in Los Angeles, California *Landscape and Urban Planning* **127** 124–35
Mohamed M *et al* 2021 Urban heat island effects on megacities in desert environments using spatial network analysis and remote sensing data: a case study from Western Saudi Arabia *Remote Sensing* **13** 1941
Mohammed A *et al* 2020 Canopy urban heat island and its association with climate conditions in Dubai *UAE. Climate* **8** 81
Moretti L *et al* 2021 Effect of sampietrini pavers on urban heat islands *Int. J. Environ. Res. Public Health* **18** 13108
Mullaney J *et al* 2015 A review of benefits and challenges in growing street trees in paved urban environments *Landscape and Urban Planning* **134** 157–66
Municipality of Athens (ed) 2017 *Athens Resilience Strategy*
Nowak D J *et al* 1996 Measuring and analyzing urban tree cover *Landscape and Urban Planning* **36** 49–57
Oke T R 1982 The energetic basis of the urban heat island *QJ Royal Met. Soc.* **108** 1–24
Peng L L H and Jim C Y 2013 Green-roof effects on neighborhood microclimate and human thermal sensation *Energies* **6** 598–618
Peng S *et al* 2012 Surface urban heat island across 419 global big cities *Environ. Sci. Technol.* **46** 696–703
Peng S and Maing M 2021 Influential factors of age-friendly neighborhood open space under high-density high-rise housing context in hot weather: A case study of public housing in Hong Kong *Cities* **115** 103231
Pomerantz M *et al* 2003 *Examples of cooler reflective streets for urban heat-island mitigation: Portland cement concrete and chip seals* Lawrence Berkeley National Laboratory (No. LBNL−−49283, 816205)
Rizwan A M *et al* 2008 A review on the generation, determination and mitigation of Urban Heat Island *J. Environ. Sci.* **20** 120–8
Roman L A *et al* 2021 Beyond 'trees are good': Disservices, management costs, and tradeoffs in urban forestry *Ambio* **50** 615–30
Roy D P *et al* 2014 Landsat-8: Science and product vision for terrestrial global change research *Remote Sens. Environ.* **145** 154–72
Santamouris M 2013 Using cool pavements as a mitigation strategy to fight urban heat island—A review of the actual developments *Renew. Sustain. Energy Rev.* **26** 224–40
SB County 2020 City limits
SBVWCD 2022 *FINAL Engineering Investigation of the Bunker Hill Basin.*
Sen S *et al* 2019 Cool Pavement Strategies for Urban Heat Island Mitigation in Suburban Phoenix, Arizona *Sustainability* **11** 4452
Shastri H *et al* 2017 Flip flop of day-night and summer-winter surface urban heat island intensity in India *Sci Rep.* **7** 40178
Shiflett S A *et al* 2017 Variation in the urban vegetation, surface temperature, air temperature nexus *Sci. Total Environ.* **579** 495–505
Skoulika F *et al* 2014 On the thermal characteristics and the mitigation potential of a medium size urban park in Athens, Greece *Landscape and Urban Planning* **123** 73–86
Smart Cities Connect 2021 *Phoenix Releases Cool Pavement Pilot Program Results.*
Sodoudi S *et al* 2014 Mitigating the urban heat island effect in megacity Tehran *Advances in Meteorology* **2014** e547974
Stewart I D and Oke T R 2012 *Local Climate Zones for Urban Temperature Studies in: Bulletin of the American Meteorological Society* **93** 1879–1900
Su J G *et al* 2009 An index for assessing demographic inequalities in cumulative environmental hazards with application to Los Angeles, California *Environ. Sci. Technol.* **43** 7626–34
Susca T *et al* 2011 Positive effects of vegetation: Urban heat island and green roofs *Environmental Pollution: Overcoming Obstacles to Sustainability and Quality of Life* 159159 *(Boston, USA, 20-23 June 2010)*
Taleghani M *et al* 2016 Micrometeorological simulations to predict the impacts of heat mitigation strategies on pedestrian thermal comfort in a Los Angeles neighborhood *Environ. Res. Lett.* **11** 024003
Transformative Climate Communities 2021 *Transformative Climate Communities.*

Turner K *et al* 2021 How are U.S. Cities Planning for Heat?
Turner V K *et al* 2022 More than surface temperature: mitigating thermal exposure in hyper-local land system *Journal of Land Use Science* **17** 79–9996
US EPA 2012 Reducing urban heat islands: compendium of strategies, Cool Pavements
US Census Bureau 2020 https://census.gov/library/stories/state-by-state/california-population-change-between-census-decade.html
USC 2017 Los Angeles Neighborhood Map | Open Data. USC Price Center https://usc.data.socrata.com/dataset/Los-Angeles-Neighborhood-Map/r8qd-yxsr
Vani V and Mandla V R 2017 Comparative Study of NDVI and SAVI vegetation Indices in Anantapur district semi-arid areas *Int. J. Civil Eng. Technol.* **8** 559–66
Wilson B 2020 Urban Heat Management and the Legacy of Redlining *J. American Planning Association* **86** 443–57
Wiltshire-Gordon S 2020 New Federal Bill Supports Heat Island Mitigation.U.S. Green Building Council https://usgbc.org/articles/new-federal-bill-supports-heat-island-mitigation
Wong M S *et al* 2016 Spatially analyzing the inequity of the Hong Kong urban heat island by socio-demographic characteristics *Int J Environ Res Public Health* **13** E317
Yamazaki F *et al* 2009 Observation of urban heat island using airborne thermal sensors *in: 2009 Joint Urban Remote Sensing Event. Presented at the 2009 Joint Urban Remote Sensing Event* 1–5
Yuan C *et al* 2020 Mitigating intensity of urban heat island by better understanding urban morphology and anthropogenic heat dispersion *Build. Environ.* **176** 106876